JOURNAL OF APPLIED ELECTROCHEMISTRY 23 (1993) 275–278

The measurement of water vapour pressure in an SOFC anode during discharge

M. NAGATA, H. IWAHARA

Synthetic Crystal Research Laboratory, School of Engineering, Nagoya University, Furo-cho, Chikusa-ku, Nagoya 464–01, Japan

Received 9 June 1992; revised 7 September 1992

By placing a galvanic-type steam sensor on the fuel electrode of a solid oxide fuel cell, water vapour pressure in the anode during discharge was successfully measured. The change in steam concentration in the anode, which was calculated from the e.m.f. of the sensor, was compared with the variation of anodic overvoltage measured by the usual d.c. interruption method. As a result, the water vapour pressure was confirmed to increase as the discharge current increased, and most of the anodic overvoltage could be ascribed to the hydrogen concentration overvoltage.

1. Introduction

Solid oxide fuel cells (SOFC) using yttria stabilized zirconia (YSZ) as an electrolyte are effective and clean energy generators. Economic operation demands that the electrode overvoltages must be small. Lanthanum strontium manganese oxide shows good characteristics as a cathode [1–3]. On the other hand, nickel zirconia cermet is usually used as an anode [4–6], but its overvoltage is often significant, even at low discharge current densities. In the anode, water vapour is produced at the three phase interface (gas, electrode and electrolyte) during discharge. If the diffusion of this water vapour is insufficient, the hydrogen concentration in the vicinity of the anode becomes lower compared to that in the bulk of the electrode compartment.

In this study a new method of measuring this hydrogen partial pressure has been developed. Water vapour pressure in the anode of a SOFC during discharge was measured by attaching a steam sensor to the electrode, the principle of which was based on a steam concentration cell using YSZ as an electrolyte, and the hydrogen partial pressure was obtained by subtracting the water vapour pressure from the total. In the present experiment, a plated platinum electrode [7] was used as a model electrode. The anodic overvoltage of the fuel cell was measured by the usual current interruption method and was compared with that calculated from the concentration of hydrogen at the anode.

2. Principle of steam sensor

The principle of a steam sensor using an oxide ion conductor will first be described. The concept of the steam concentration cell is illustrated schematically in Fig. 1 [8, 9]. When hydrogen with different humidity is introduced into each electrode compartment, the cell generates an e.m.f. depending on the difference in the partial pressure of the water vapour, that is the cell

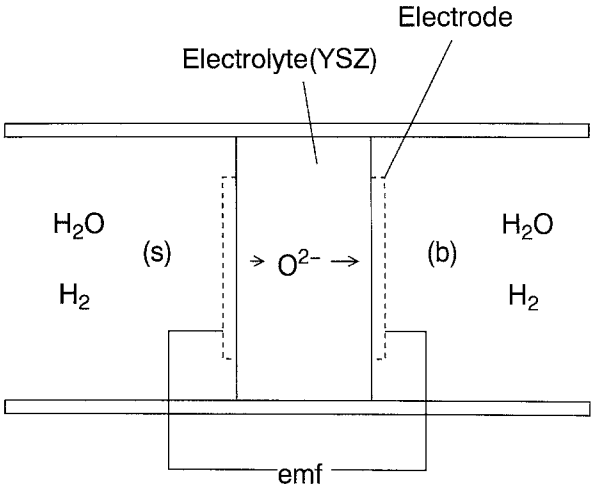

Fig. 1. Concept of steam concentration cell using oxygen ion conductor.

works as a steam concentration cell, as illustrated in Fig. 1. The electrode with higher humidity is the cathode in this cell. The electrode reactions of this cell are as follows:

$$\text{Anode: } H_2 + O^{2-} \longrightarrow H_2O + 2e^- \quad (1)$$

$$\text{Cathode: } H_2O + 2e^- \longrightarrow H_2 + O^{2-} \quad (2)$$

The theoretical e.m.f. of the cell is given by

$$E = \frac{RT}{2F} \ln \frac{P_b(H_2O)P_s(H_2)}{P_s(H_2O)P_b(H_2)} \quad (3)$$

where $P_s(H_2)$ and $P_b(H_2)$ are the partial pressure of hydrogen, $P_s(H_2O)$ and $P_b(H_2O)$ are the water vapour pressure in compartments s and b, respectively, and R, T and F have their usual meanings. In the present experiment, 's' refers to the surface of the anode and 'b' means the bulk of the anode gas phase as shown in Fig. 2. Since the plated platinum electrode is thin enough (2–3 μm) for the gas to diffuse quickly, the total gas pressure in the anode can be assumed to be 1 atm. Because the gas diffusion in the bulk is also fast,

0021-891X © 1993 Chapman & Hall

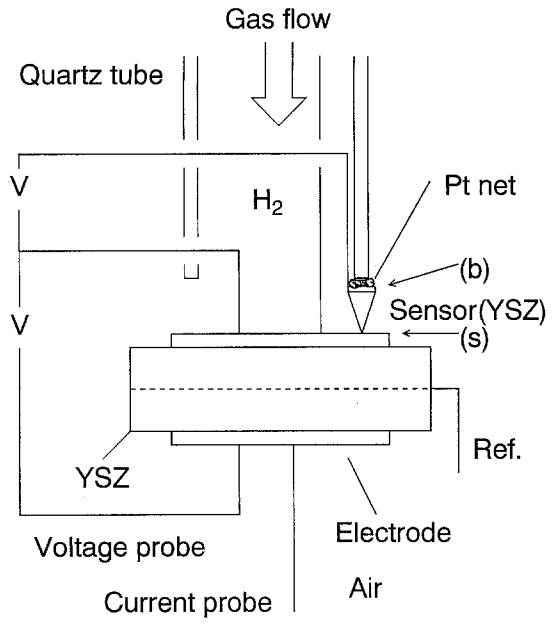

Fig. 2. Schematic diagram of the test cell in which the steam sensor was attached to the anode.

the following equations can be obtained:

$$P_s(H_2O) + P_s(H_2) = 1 \quad (4)$$

$$P_b(H_2O) + P_b(H_2) = 1 \quad (5)$$

From Equations 3, 4 and 5, Equation 6 can be derived:

$$P_s(H_2O) = \frac{P_b(H_2O)}{P_b(H_2O) + P_b(H_2)\exp(2EF/RT)} \quad (6)$$

Using this equation, the water vapour pressure can be estimated from the e.m.f. E of the sensor, because the partial pressure of each component in the bulk is known.

3. Experimental details

A hydrogen–air fuel cell was constructed with nonelectrolytically plated platinum electrodes (0.5 cm^2 working area) using a disc-shaped YSZ (TZ-8Y) electrolyte (13 mm diam.). The thickness of the plated platinum was 2–3 μm, and the films show almost the same morphology and same electrode characteristics under fixed preparation conditions. The properties of plated platinum as a cathode and anode of a SOFC have been described elsewhere [7]. A reference electrode (platinum wire) was wound laterally around the electrolyte disc to measure the anodic and cathodic overvoltages independently.

The pyramid-shaped steam sensor element (which was made of YSZ with a base area of 1.5 mm × 3 mm and a height of 4 mm) was attached to the fuel electrode by means of a quartz tube as schematically shown in Fig. 2. The purpose of its shape was to avoid impeding the diffusion of the water vapour from the anode. On the base of the pyramid, the platinum electrode was attached by electroless plating as a standard gas electrode. Instead of using both a sensing electrode and a standard gas electrode, only the plated platinum anode was attached to the apex to measure the correct value of the water vapour pressure in the electrode.

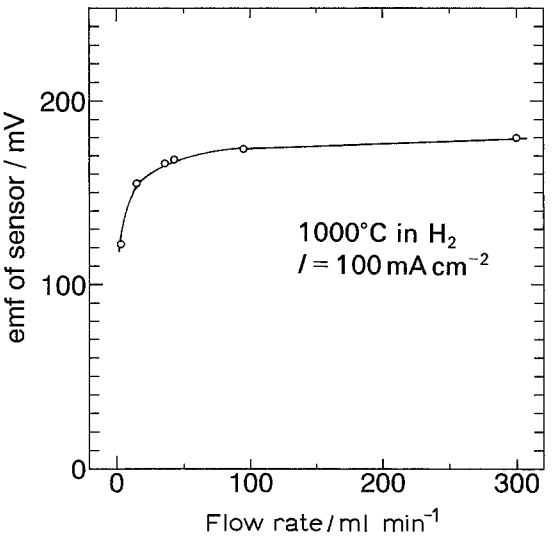

Fig. 3. The dependence of the e.m.f. of the steam sensor on gas flow rate.

Overvoltage was measured by the usual current interrupting method (Nikko Keisoku current pulse generator NCPG-101). The cell was operated at 1000 °C. Hydrogen gas saturated with water at room temperature (29 °C) flowed from the inside of the quartz tube to the outside, passing along the pyramid-shaped sensor.

4. Results and discussion

The dependence of the e.m.f. of the steam sensor on the gas flow rate in the fuel cell under operation was examined first. As shown in Fig. 3, the e.m.f. of the sensor became almost constant above a flow rate of 50 ml min^{-1} of hydrogen at 100 mA cm^{-2}. Such dependency was also tested at a current density of 500 mA cm^{-2} and it was confirmed that the e.m.f. was almost constant at a flow rate higher than 50 ml min^{-1}. The following experiments were carried out under a gas flow rate of 60 ml min^{-1}.

The fuel cell was discharged and the e.m.f. of the steam sensor as well as the overvoltage of the cell were measured. The water vapour pressure was calculated from Equation 6 and the measured e.m.f. The results were plotted against the discharge current density in Fig. 4(a) and this was compared with anodic overvoltage (Fig. 4b) measured by the usual current interruption method. From these diagrams it is clear that the increase of water vapour pressure in the anode directly causes significant overvoltage at the anode. In Fig. 5, anodic overvoltage was plotted against water vapour pressure. A rapid increase of the anodic overvoltage can be seen with the increase in water vapour pressure.

The hydrogen gas pressure in the anode ($P_s(H_2)$) during discharge was calculated assuming Equation 4 and was plotted against the discharge current. As shown in Fig. 6, the partial pressure of hydrogen in the anode decreases almost linearly with the discharge current up to 0.3 A cm^{-2}, after which the slope becomes less steep. This behaviour may be explained by considering Knudsen mutual diffusion of hydrogen

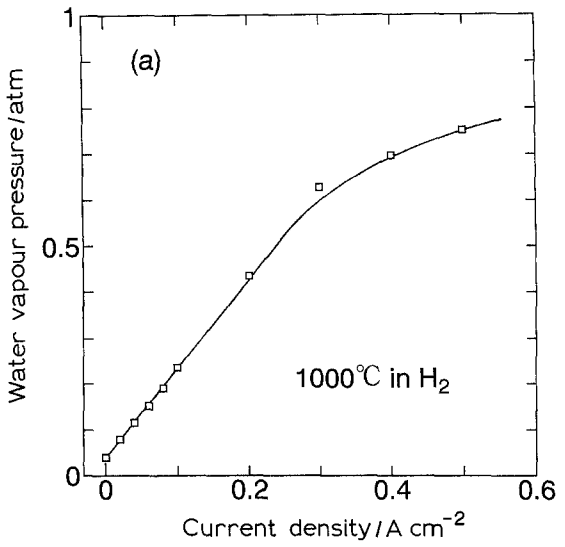

Fig. 4. (a) Water vapour pressure, and (b) anodic overvoltage during discharge.

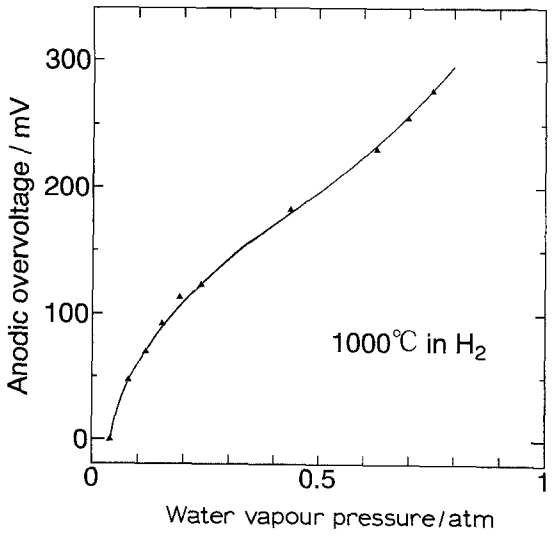

Fig. 5. Anodic overvoltage against water vapour pressure in the anode.

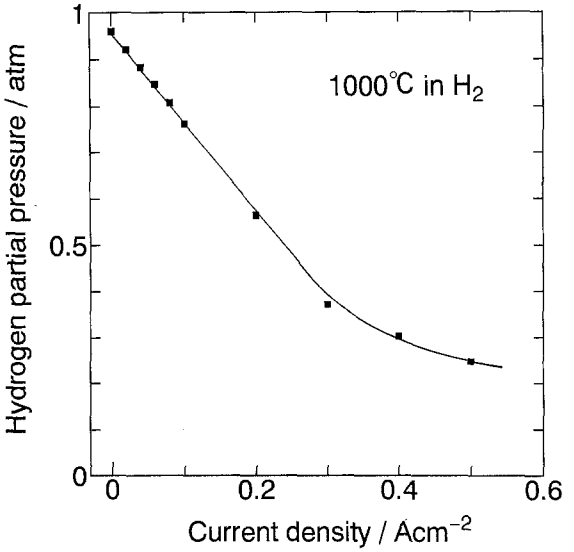

Fig. 6. Hydrogen partial pressure in the anode during discharge.

and steam, although a quantitative discussion requires precise data of diffusion coefficients and complex mathematical procedures.

Concentration overvoltage due to hydrogen diffusion was calculated from the values shown in Fig. 6 using Equation 7, and it was compared with an anodic overvoltage of the SOFC measured by the current interruption method.

$$\eta = \frac{RT}{2F} \ln \frac{P_s(H_2)}{P_b(H_2)} \qquad (7)$$

As shown in Fig. 7, it is clear that most (85–90%) of the anodic overvoltage is caused by the hydrogen concentration overvoltage.

The e.m.f. decay of the sensor was measured to prove the assumption of Equation 4 (i.e. the total pressure in the anode is always 1 atm) and also to prove that the apex of the sensor did not impede the gas diffusion from the electrode. If the sensor element inhibited the gas diffusion from the electrode, the e.m.f. decay would slow when the discharge current was cut. In our experiment, as shown in Fig. 8, the

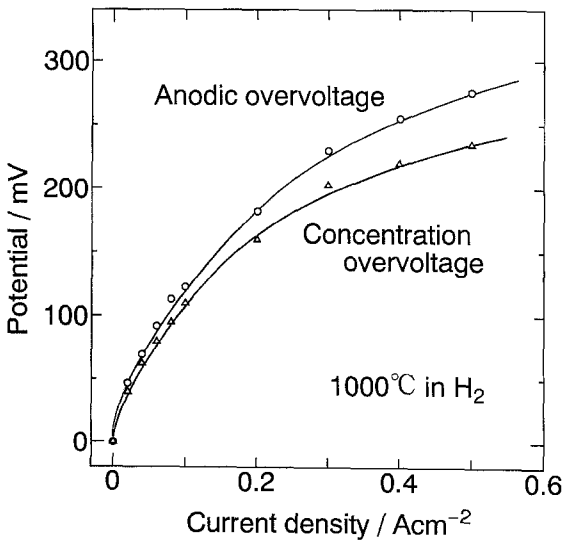

Fig. 7. Plots of overvoltages against discharge current density.

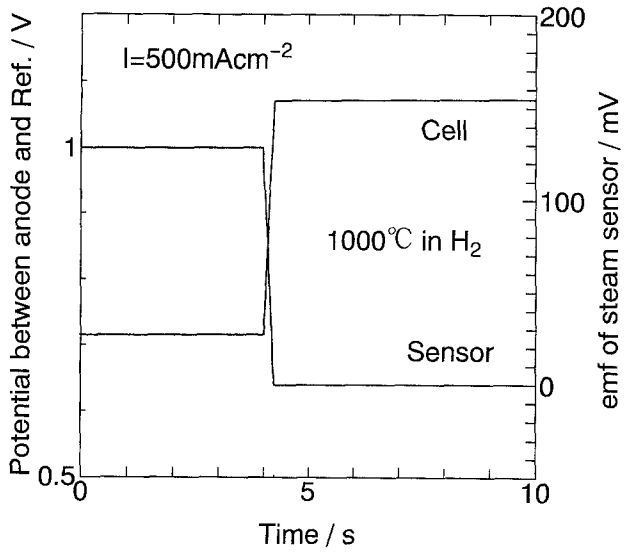

Fig. 8. Decay curves of potentials of the steam sensor and the cell.

e.m.f. of the sensor became zero within a time of 20 ms after the discharge was stopped. From this result, it is recognized that the sensor does not impede the diffusion of water vapour from the anode and that the assumption of Equation 4 is correct (i.e. the gas diffusion in the electrode is sufficient enough).

5. Conclusion

This paper has presented a new method for measuring the water vapour pressure in the anode of SOFC during discharge using a steam sensor. The e.m.f. of the steam sensor responded well to the change in the anodic potential of the fuel cell. Hydrogen partial pressure in the anode could also be estimated by subtracting the water vapour pressure from the total. Most of the anodic overvoltage was ascribed to the hydrogen concentration overvoltage. Measurement of water vapour pressure in the Ni–YSZ cermet, which is a practical anode of SOFC, remains to be performed.

References

[1] K. Tsuneyoshi, K. Mori, A. Sawata, J. Mizusaki and H. Tagawa, *Solid State Ionics* **35** (1989) 263–8.
[2] O. Tamamoto, Y. Takeda, R. Kannno and M. Noda, *ibid.* **22** (1987) 241.
[3] A. Hammouche, E. Siebert, A. Hammou and M. Kleitz, *J. Electrochem. Soc.* **138** (1991) 1212.
[4] H. Tanabe and S. Fukushima, *Electrochim. Acta*, **31** (1986) 801–9.
[5] K. Tanemura and F. Umemura, *Denkikagaku* **58**(10) (1990) 896–900.
[6] T. Kawada, N. Sakai, H. Yokokawa and Dokiya, *Solid State Ionics* **40/41** (1990) 402–6.
[7] M. Nagata, T. Esaka and H. Iwahara, *Denkikagaku* **59**(8) (1991).
[8] H. Iwahara, T. Esaka, H. Uchida and N. Maeda, *Solid State Ionics*, **3/4** (1981) 359.
[9] H. Uchida, N. Maeda and H. Iwahara, *J. Appl. Electrochem.* **12** (1982) 645.